REGULATORY ARCHITECTURE OF GENE EXPRESSION VARIATION IN THE THREESPINE STICKLEBACK, *GASTEROSTEUS ACULEATUS*.

Victoria L. Pritchard [1], Heidi M. Viitaniemi [1,2], R.J. Scott McCairns [2,5], Juha Merilä [2], Mikko Nikinmaa [1], Craig R. Primmer [1] & Erica H. Leder [1,3,4].

[1] Division of Genetics and Physiology, Department of Biology, University of Turku, Turku, Finland

[2] Department of Biosciences, University of Helsinki, Helsinki, Finland.

[3] Natural History Museum, University of Oslo, Norway

[4] Institute of Veterinary Medicine and Animal Sciences, Estonian University of Life Sciences, Tartu, Estonia

[5] Institut Méditerranéen de la Biodiversité et d'Ecologie Marine et Continentale, Marseille, France.

Abstract

Much adaptive evolutionary change is underlain by mutational variation in regions of the genome that regulate gene expression rather than in the coding regions of the genes themselves. An understanding of the role of gene expression variation in facilitating local adaptation will be aided by an understanding of underlying regulatory networks. Here, we characterize the genetic architecture of gene expression variation in the threespine stickleback (*Gasterosteus aculeatus*), an important model in the study of adaptive evolution. We collected transcriptomic and genomic data from 60 half-sib families using an expression microarray and genotyping-by-sequencing, and located QTL underlying the variation in gene expression (eQTL) in liver tissue using an interval mapping approach. We identified eQTL for several thousand expression traits. Expression was influenced by polymorphism in both *cis* and *trans* regulatory regions. *Trans* eQTL clustered into hotspots. We did not identify master transcriptional regulators in hotspot locations: rather, the presence of hotspots may be driven by complex interactions between multiple transcription factors. One observed hotspot co-located with a QTL recently found to underlie salinity tolerance in the threespine stickleback. However, most other observed hotspots did not co-locate with regions of the genome known to be involved in adaptive divergence between marine and freshwater habitats.

Introduction

It is now known that much adaptive evolution is underlain by changes in regions of the genome regulating gene expression, rather than in the protein coding regions of the genes themselves (Pavey *et al.* 2010). Recent work has demonstrated that much variation in gene expression is heritable, and thus evolvable via selection (e.g. Ayroles *et al*. 2009, Powell *et al.* 2013, Leder *et al.* 2015). Correspondingly, studies using model species have found that the genetic polymorphisms underlying phenotypic variation are typically not within genes (Flint and Mackay 2009). Variation in gene expression has been shown to underlie several well-documented cases of phenotypic and/or adaptive divergence. These include plumage coloration and beak shape in birds (Mallarino *et al.* 2011; Poelstra *et al.* 2015), mimetic wing patterns in butterflies (Reed *et al.* 2011; Hines *et al.* 2012), and flower colour (Durbin *et al.* 2003). Further, differences in gene expression patterns have been found to correlate with adaptive divergence in multiple species (e.g. Bernatchez *et al.* 2010; Barreto *et al.* 2011). Dysregulation of gene expression due to interactions amongst regulatory loci has potential to cause reduced fitness of inter-population hybrids and thus contribute to reproductive isolation (Ellison and Burton 2008; Turner *et al.* 2014). However, it may also promote hybrid speciation by enabling hybrids to exploit new niches (Lai *et al.* 2006).

The genetic architecture of gene expression regulation can be investigated by treating expression variation as a quantitative trait and identifying the genomic locations associated with it (termed 'expression quantitative trait loci' or 'eQTL'). Such studies have shown that the expression of a gene can be regulated by multiple genomic regions, which are traditionally classified as either *cis* or *trans*. *Cis* regulators, including promoters that activate transcription and enhancers that influence transcription levels, are located close to the regulated gene(s). They contain binding sites for regulatory molecules (proteins or mRNA) that are produced by more distant, *trans*, regulators. As *cis* regulators are expected to affect only one or a few focal genes, while *trans* regulators may have pleiotropic effects on many genes, *cis* and *trans* regulators are subject to different evolutionary dynamics. *Cis* regulatory changes are expected to be important drivers of local adaptation (Steige *et al.* 2015), while *trans* regulatory variation is considered more likely to be under purifying selection (Schaefke *et al.* 2013 but see also Landry *et al.* 2005 for discussion of *cis-trans* coevolution). Correspondingly, *trans* regulatory polymorphisms tend to affect gene expression less strongly than *cis* polymorphisms, and their effects are more likely to be non-additive (Zhang *et al.* 2011; Gruber *et al.* 2012; Schaefke *et al.* 2013; Meiklejohn *et al.* 2014; Metzger *et al.* 2016). Nevertheless, work in multiple species has demonstrated an important role for both *cis* and *trans* polymorphism in shaping expression variation (Cubillos *et al.* 2012; Meiklejohn *et al.* 2014; Guerrero *et al*. 2016) and the role of *trans* variation may have been underestimated due to the higher statistical power required to detect it (Mackay *et al.* 2009; Clément-Ziza *et al.* 2014). Interactions involving *trans* regulators may be particularly important in reducing the fitness of inter-population hybrids (Turner *et al.* 2014).

Supporting the pleiotropic role of *trans* regulators, a ubiquitous feature of eQTL studies is the identification of '*trans* eQTL hotspots', genomic locations associated with expression variation in many distant genes which are thought to harbour one or more important *trans* regulators (Wu *et al.* 2008; Clément-Ziza *et al.* 2014; Meiklejohn *et al.* 2014).

The threespine stickleback (*Gasterosteus aculeatus*) is an important model in the study of adaptive evolution. Ancestral anadromous populations of threespine stickleback have repeatedly and independently colonized freshwater throughout the Northern Hemisphere (Taylor and McPhail 2000; Mäkinen *et al.* 2006). Sympatric and parapatric freshwater populations may exploit different habitats (Schluter and McPhail 1992; Roesti *et al.* 2012). The species is also distributed throughout semi-marine environments with large temperature and salinity gradients, such as estuaries and the brackish water Baltic Sea (McCairns and Bernatchez 2010; Guo *et al.* 2015; Konijnendijk *et al.* 2015). Successful colonization of these diverse habitats necessitates behavioural, morphological and physiological adaptation to novel environmental conditions including changed temperature, salinity, oxygen, light, parasite and predator regimens, a process that can occur rapidly (Kitano *et al.* 2010; Barrett *et al.* 2011; Terekhanova *et al.* 2014; Lescak *et al.* 2015; Huang *et al.* 2016, Rennison *et al.* 2016). Parallel adaptations between independently founded freshwater populations frequently involve the same regions of the genome and arise from pre-existing genetic variation in the marine population (Colosimo *et al.* 2005; Hohenlohe *et al.* 2010; Jones *et al.* 2012; Liu *et al.* 2014; Conte *et al.* 2015, but see DeFaveri *et al.* 2011; Leinonen *et al.* 2012; Ellis *et al.* 2015; Ferchaud and Hansen 2016). Local adaptation in environmentally heterogeneous habitats such as the Baltic Sea (Guo *et al.* 2015) and lake-stream complexes (Roesti *et al.* 2015) has been shown to involve the same genomic regions. Evidence suggests that much of this adaptation may be due to changes in gene regulation rather than protein structure (Jones *et al.* 2012). In addition, plasticity in gene expression in response to different environmental conditions may facilitate initial colonization of novel habitats.(McCairns and Bernatchez 2010; Morris *et al.* 2014). Leder *et al.* (2015) recently demonstrated substantial heritability of expression variation, over thousands of genes, within a Baltic Sea threespine stickleback population, confirming that it can be shaped by local selection. One well-documented locally adaptive trait, reduction of the pelvic girdle, is known to be underlain by variation in the *cis* regulatory region of the *Pitx1* gene (Chan *et al.* 2010), and *cis*-regulatory variation at the *Bmp6* gene underlies divergent tooth number between a freshwater and marine population (Cleves *et al.* 2014). Differences in levels of thyroid hormone between freshwater and marine sticklebacks, which are connected to different metabolic rates between the two environments, are associated with *cis* regulatory variation at the *TSHβ2* gene (Kitano *et al.* 2010). Recently, Di Poi et al (2016) showed that differences in behaviour and response to stress between marine and freshwater sticklebacks may be modulated by variation in the expression of hormone receptors. Otherwise, the architecture of gene

expression regulation in the threespine stickleback and its role in adaptive evolution is only starting to be explored (Chaturvedi *et al.* 2014).

Understanding the regulatory pathways underlying variation in gene expression, and how this gene expression variation influences the phenotype, will improve our understanding of how organisms can adapt to novel environments and, thus how adaptive diversity is generated. In the stickleback, for example, it is unknown whether regulatory loci involved in local adaptation are clustered on the regions of the genome that show repeated divergence in independent marine-freshwater colonizations. Here, we perform the first genome-wide study of this regulatory architecture in the threespine stickleback, by mapping QTL underlying the variation in expression of several thousand genes in a population from the Baltic Sea. We examine transcription in the liver, a metabolically active tissue that expresses many genes potentially involved in physiological adaptation to different aquatic habitats.

Methods

Experimental crosses.

We used a multi-family paternal half-sib crossing design for QTL mapping. Crossing procedures have previously been detailed in Leinonen *et al.* (2011) and Leder *et al.* (2015). In short, 30 mature males and 60 gravid females were collected from the Baltic Sea for use as parents. Each male was artificially crossed with two females, producing 30 half-sib blocks each containing two full-sib families. Families were reared in separate 10L tanks with density standardized to 15 individuals per tank, temperature at 17 ± 1°C and 12:12h light/dark photoperiod. At the age of six months, ten offspring from each family (5 treated, 5 controls) were subject to a temperature treatment as part of a related experiment (control: constant 17°C; treatment: water gradually heated from 17°C to 23°C over 6 hours, see Leder *et al.* 2015), and immediately euthanized for DNA and RNA collection.

RNA preparation, microarray design, and data normalization

RNA preparation, gene expression microarrays, hybridization, and normalization procedures are described in detail in Leder *et al.* (2009, 2015). Briefly, total RNA was isolated from offspring liver tissue using standard protocols. RNA that passed quality thresholds was labelled (Cy3 or Cy5) using the Agilent QuickAmp Kit, with equal numbers of individuals within family groups (control & temperature-treated; males & females) assigned to each dye. Labelled RNA was hybridized to a custom 8x15K microarray, with sample order randomized (Agilent Hi-RPM kit). Labelling, hybridization, and scanning was performed at the University Health Network in Toronto, Canada. Images of the arrays were acquired, image analysis was performed, and array quality was assessed as detailed in Leder *et al.* (2015). Post-processed signals were standardized across arrays using a

supervised normalization approach, implemented in the package 'snm' for R/Bioconductor (Mecham *et al.* 2010; R Core Team 2015). Dye, array and batch (i.e. slide) were defined as 'adjustment variables'; sex, family and temperature treatment were defined as 'biological variables'. Following normalization, individual intensity values more than two standard deviations from their family-by-treatment mean, and probes with missing values for an entire family or >10% of individuals were removed. The final dataset contained 10,527 expression traits (10,495 genes plus 32 additional splice variants) and 563 individuals (158 control females; 125 control males; 152 treated females; 128 treated males).

Genotyping-by-Sequencing

For genotyping-by-sequencing of parents (n = 90) and offspring (n = 580) we used the method of Elshire *et al.* (2011) with an additional gel excision step to improve size selection. DNA was extracted from ethanol preserved fin tissue (parents) or frozen liver tissue (offspring) and DNA concentrations were measured using a NanoDrop ND-1000 spectrophotometer. DNA (80 ng) was digested with the restriction enzyme Pst1 1.5 U (New England Biolabs) and 1x NEB buffer 3, 1x bovine serum albumin (BSA) and dH_2O (3.3 µl) in a thermocycler (37°C, 2h; 75°C, 15min; 4°C, 10min). The digested DNA was ligated to adapters with T4-ligase 0.6x (New England Biolabs), 1x Ligase Buffer, 21 µl dH_2O and 50 nM of pooled forward and reverse adapters, which were prepared according to Elshire *et al.* (2011; ligation program: 22°C, 1h; 65°C, 30min; 4°C, 10min). Up to one hundred and four unique barcodes were used in each library to label individual samples. The ligation products were pooled into libraries and purified with a QIAquick PCR Purification Kit (Qiagen). The purified libraries were PCR amplified with the following components: Purified ligated library (20µl), reaction buffer 1x, $MgCl_2$ 1.5nM (Bioline), primer mix 0.5 µM, dNTPs (Fermentas) 0.4µM, BioTaq 0.05 U (Bioline) and dH_2O (20µl) (Amplification program: [72C°, 5min; 4 cycles [95°C, 30s; 95°C, 10s; 65°C, 30s; 70°C, 30s]; 11 cycles [95°C, 10s; 65°C, 30s; 72°C, 20s]; 72°C, 5min; 4°C, 10min). Lastly, we performed a manual size selection by loading 40 µl of the amplified library on a gel (MetaPhor [Lonza] 2.5 %, 150 ml, 100 V. 1.5 h) and cutting the 300-400 bp range from the resultant smear. The DNA was extracted from the gel with a QIAquick Gel Extraction Kit (Qiagen). The cleaned product was again separated on a gel, cut and cleaned.

All products were sequenced with paired-end reading on the Illumina HiSeq2000 platform. Six hundred and fifty individuals, multiplexed into ten separate libraries (maximum library size = 104 individuals), were sequenced at the Beijing Genomics Institute (BGI); 55 individuals (including duplicates) were sequenced at the Finnish Institute for Molecular Medicine or at the University of Oslo.

Variant calling

Reads were split by barcode, and barcodes removed, using a custom perl script. Low quality bases were removed from the reads via window adaptive trimming using Trim.pl (available: http://wiki.bioinformatics.ucdavis.edu/index.php/Trim.pl, Illumina quality score ≤ 20). Paired-end reads for each of these individuals were aligned to the BROAD S1 stickleback genome using BWA aln/sampe (v 0.6.2) with default parameters (Li and Durbin 2009). The threespine stickleback genome comprises 21 assembled chromosomes plus 1,823 un-placed genomic scaffolds. Unmapped reads, and reads with non-unique optimal alignments, pair-rescued alignments, or any alternative suboptimal alignments, were discarded from resulting SAM files. SAM files were converted to sorted BAM files using samtools 0.1.18 (Li *et al.* 2009) and variants were called within each paternal family using the samtools mpileup function with extended BAQ computation (options: -AED, max-depth 500), in combination with bcftools (Li *et al.* 2009). We did not degrade mapping quality for reads with large numbers of mismatches as we found this to reject high-quality reads due to fixed polymorphisms between our European stickleback samples and the North American stickleback genome. Indel and multi-allelic variants were discarded. Initial filters based on SNP quality and variability within and across families resulted in list of 26,290 candidate bi-allelic SNPs for further analysis. Samtools and bcftools, applied to each paternal family separately, were then used to call each individual for the genotype at each of the 26,290 sites. Sites at which bcftools identified multiple variant types (SNPs, indels and multi-base polymorphisms) within and among families were removed, leaving 25,668 successfully genotyped variant sites.

Genotype quality control

Vcftools (Danecek *et al.* 2011) was used to recode genotypes with a genotype quality phred score (GQ) < 25 or a sequencing depth (DP) < 8 or > 1000 to missing. Vcf files for all families were merged and the merged file converted to the input format for Plink 1.07 (Purcell *et al.* 2007). For SNPs on all autosomal chromosomes and the pseudoautosomal region of Chromosome 19 (see below), the following filters were applied in Plink: hwe (based on founders only) < 0.01, maximum missing genotypes = 0.25, minor allele frequency > 0.05, offspring with > 70% missing data removed. Adjacent SNPs in complete linkage disequilibrium were manually consolidated into a single locus, with combined SNP information used to call genotypes.

Several approaches were used check for sample contamination or errors in barcode splitting and family assignment: in Plink, the *mendel* option was used to screen families for Mendelian errors, and sample relatedness was examined by graphically visualizing genome-wide IBD-sharing coefficients generated by *genome*; the program SNPPIT (Anderson 2012) was used to assign individuals to parents, based on five independent datasets of 100 SNPs; and 220 SNPs on Stratum II of Chromosome 19 (see below) were examined for their expected pattern in males and females (all heterozygous in males vs. all homozygous in females).

The stickleback Chromosome 19 is a proto-sex chromosome (Peichel *et al.* 2004; Roesti *et al.* 2013; Schultheiß *et al.* 2015), with a normally recombining pseudo-autosomal domain (approximately 0-2.5mB), a non-recombining domain in the male version (Stratum I, approximately 2.5-12mB) and a domain largely absent in the male version (Stratum II, approximately 12-20mB). For Stratum I, parental and offspring genotypes were inspected manually in order to identify the male-specific allele and this was recoded to a unique allele code ('9') for the purposes of linkage map construction. Where the male-specific allele could not be identified, all genotypes within a family were re-coded as missing. Genotypes were also inspected manually for Stratum II, and any SNP found to be heterozygous in males was excluded. All remaining Stratum II SNPs were considered to be hemizygous in males, and one of the alleles was also recoded as '9'.

Linkage map construction

We constructed a linkage map using the improved version of Crimap (Green *et al.* 1990, available: http://www.animalgenome.org/tools/share/crimap/). Remaining Mendelian errors in the dataset were removed using the *set-me-missing* option in Plink. For each SNP, the number of informative meiosis was examined using Crimap, and markers with < 150 informative meioses or within 500bp of one another were discarded.

The initial map build included 6,448 markers. Where applicable, SNPs were ordered according to the modified genome build of Roesti *et al.* (2013). We attempted to position all previously un-placed scaffolds containing at least two genotyped SNPs on to the map. Scaffolds were assigned to chromosome on the basis of LOD score using the Crimap function *two-point*, and then positioned using a combination of information from pilot Crimap *builds*, *chrompic*, and *fixed* together with known start and end points of previously assembled scaffolds (Roesti *et al.* 2013). Information from *chrompic* and *fixed* were also used to confirm the orientation of scaffolds newly placed by Roesti *et al.* (2013). Once all possible scaffolds had been placed, recombination distance between ordered SNPs was estimated using *fixed*. To refine the map, we iteratively removed SNP genotypes contributing to implied double crossovers within a 10 cM interval (presumed to be genotyping errors), and SNPs generating recombination distances of >1cM per 10,000 bp and recalculated distances using *fixed*. Remaining regions of unusually high recombination on the map were investigated by examining whether removal of individual SNPs altered map distance.

eQTL identification

Expression QTL (eQTL) were identified using an interval mapping approach (Knott *et al.* 1996) implemented in QTLMap 0.9. 0 (http://www.inra.fr/qtlmap; QTLMap option: -- *data-transcriptomic*). Offspring with missing genotypes at > 60% of the markers in the linkage map were removed from the analysis. We applied linkage analysis assuming a Gaussian trait distribution (QTLMap option: --

calcul = 3), and included dye, temperature treatment, and sex as fixed factors in the model. Due to the relatively small size of some of our half-sib families, we examined sire effects only, with a separate QTL effect estimated for each sire. Excluding dam effects is expected to reduce our power of eQTL detection, as fewer parents will be segregating for each QTL.

A fast algorithm was used to identify phase and estimate transmission probabilities at each chromosomal location (Elsen *et al.* 1999, QTLMap option: --*snp*). Autosomes and the pseudoautosomal portion of the sex chromosome were scanned at 1cM intervals, and the presence of QTL on a chromosome was assessed using a likelihood ratio test (LRT) under the hypothesis of one versus no QTL. Chromosome-wide LRT significance thresholds for each trait were identified empirically, by permuting fixed effects and traits amongst individuals within families and recalculating LRT scores (5000 permutations). As the combination of 5000 permutations x 10,332 traits x 21 chromosomes was computationally prohibitive, we first performed permutations on a subset of 200 expression traits to establish a LRT threshold below which identified QTL were unlikely to be significant at chromosome-wide $p < 0.05$ (LRT = 55), and then used permutations to assess significance of all QTL above this threshold. The non-pseudo-autosomal region of the female Chromosome 19 can be considered analogous to the X chromosome; identification of QTL in this region requires estimation of dam effects and was therefore not performed. The 95% confidence interval for each QTL was estimated using the drop-off method implemented in QTLMap 0.9.7, which returns flanking map positions plus their nearest marker.

Cis vs. trans eQTL

To discriminate *cis* vs. *trans* QTL, we compared inferred QTL location to the position of the expressed gene according to the BROAD *G. aculeatus* genome annotation v. 1.77 (available: http://ftp.ensembl.org/pub/release-77/gtf/gasterosteus_aculeatus/). All positions on the BROAD annotation were re-coded to positions on our modified chromosome assemblies. For genes on scaffolds un-anchored to our assembly, we also used information on chromosomal scaffold locations available in the recently published map of Glazer *et al.* (2015). Any eQTL on a different chromosome from the regulated gene was considered *trans*. For eQTL on the same chromosome as the gene, we initially considered two alternative threshold distances for an eQTL to be considered *trans* (> 1Mb following Grundberg *et al.* 2012, or > 10Mb following van Nas *et al*. 2010). For the 1Mb threshold, we observed strong enrichment of significant *trans* eQTL on the same chromosome as the regulated gene, indicating that these were actually mis-identified *cis* eQTL; we therefore selected the conservative 10Mb threshold. In practice, examination of our results showed that 95% CI of eQTL sometimes extended further than this 10Mb threshold. Considering median 95% CI (approximately 1Mb), we therefore classified a QTL as *trans* if the SNP closest to the upper or lower 95% confidence bounds of that QTL was further than 9.5Mb from the regulated gene. Following Johnsson *et al.* (2015)

we applied a local significance threshold (chromosome-wide $p < 0.01$) for evaluation of possible *cis*-QTL and a genome-wide significance threshold (genome-wide $p < 0.021$, = chromosome-wide threshold of 0.001 * 21 chromosomes) for evaluation of possible *trans*-QTL. Although this significance threshold is permissive, we considered it acceptable as our aim was to analyse the eQTL distribution across the genome rather than to identify individual QTL-locus associations. Similar significance thresholds have been used for eQTL detection in comparable studies (e.g. Whiteley *et al.* 2008).

To ask whether the effect of variation in *trans* regulatory sites was more often non-additive than the effect of variation in *cis* regulatory sites, we examined the narrow sense heritability (h^2) and dominance proportion of genetic variance (d^2) estimated for each expression trait by Leder *et al.* (2015) and provided in the Supplementary Data for that paper.

Genes with plastic vs. non-plastic expression

To investigate whether genes exhibiting an alteration in expression level in response to a temperature stress treatment (i.e. those exhibiting environmental plasticity) had a different underlying regulatory architecture to those not exhibiting such a response, we divided genes into a 'responding' and 'non-responding' group based on the results provided in the Supplementary Data for Leder *et al.*(2015) and compared the frequency and position of *cis* and *trans* eQTL between the two groups.

Evaluation of eQTL hotspots

As all identified eQTL had wide 95% confidence intervals, meaning that physically close eQTL positions could be due to the effect of the same locus (see below), we evaluated potential eQTL hotspots by counting eQTL within 5cM bins across the genome ('hotspot size' = number of eQTL). Where the number of 1cM bins within a chromosome was not a simple multiple of 5, bin sizes at the start and/or end of the chromosome were increased to 6 or 7. To obtain an empirical significance threshold above which clusters of eQTL could be considered a 'hotspot', we simulated the expected neutral distribution of eQTL across the genome using a custom script. We performed 5000 simulations: for each, we assigned *n* eQTL (where *n* = relevant number of significant eQTL) randomly across the 3,062 1cM bins of the genome and then summed them into 5cM (or larger) bins as described above. Conservatively, we compared the size of hotspots in the real data to the size distribution of the largest hotspot observed over each of the 5000 simulations.

Association of eQTL with regions under selection

Hohenlohe *et al.* (2010), Jones *et al.* (2012), and Terekhanova *et al.* (2014) documented parallel regions of the genome divergent between marine and freshwater sticklebacks on Chromosomes 1, 4 (three regions), 7, 11 and 21. We investigated whether these regions harboured important *trans*

regulators that might contribute to adaptation to different aquatic habitats by comparing the location of these regions with the location of our identified *trans* eQTL hotspots. We also compared hotspot location to regions of the genome inferred by Guo *et al.* (2015) to be involved in adaptive differentiation amongst different stickleback populations in the Baltic Sea.

Ortholog identification

In order to maximize the functional information available, we identified human orthologues for *G. aculeatus* genes. As a first attempt, we used BioMart (Durinck *et al.* 2005; Smedley *et al.* 2009) to identify human orthologues and obtain the HGNC symbols for the human genes. When BioMart failed to return a human orthologue, protein BLAST searches were used to identify orthologues using the Ensembl human protein database. The identifier conversion tool, db2db, from bioDBnet (https://biodbnet-abcc.ncifcrf.gov/db/db2db.php) was used to convert between Ensembl identifiers and HGNC gene symbols when needed (Mudunuri *et al*. 2009).

Hotspot annotation

To identify regulatory genes physically associated with an eQTL hotspot, we defined hotspot confidence boundaries as being the most frequently observed 95% confidence limits of all significant eQTL centred in the hotspot. We used AmiGO2 (Carbon et al. 2009) to identify 'molecular function' or 'biological process' Gene Ontology (GO) terms associated with transcriptional regulation by applying the search term [transcription regulation and – pathway]. We then used BioMart to examine all genes within the hotspot boundaries for any of these GO annotations, using the HGNC symbols as input. As an important transcriptional regulator generating a hotspot might itself be regulated by the hotspot rather than physically present within it, we repeated this analysis for all genes with eQTL mapped to the hotspot (*cis* eQTL significant at chromosome-wide $p < 0.01$; *trans* eQTL significant at genome wide $p < 0.021$). We used DAVID (Huang *et al.* 2009a; b).to examine GO term enrichment for the sets of genes with *trans* QTL mapping to each hotspot, using the 9,071 genes on the microarray with identified human orthologues as the background. To increase our sample size, we lowered our stringency and examined all genes with *trans* eQTL mapping to the hotspot locations at genome-wide $p < 0.057$ (chromosome-wide $p < 0.0027$).

Upstream regulator and functional interaction analyses

To search for regulatory genes which may be responsible for the expression variation in genes with identified *trans* eQTL, we used the upstream regulator analysis in the Ingenuity Pathway Analysis (IPA) software (Qiagen). This analysis uses a Fisher's Exact Test to determine whether genes in a test dataset are enriched for known targets of a specific transcription factor. We used the human HGNC symbols as identifiers in IPA. First we examined all genes that had a significant *trans*- eQTL mapping to any location at a genome-wide $p < 0.021$ (chromosome –wide $p < 0.001$). To investigate in more

detail the upstream regulators potentially involved in generating eQTL hotspots, we lowered our stringency and also examined all genes with *trans* eQTL mapping to the hotspot locations at genome-wide $p < 0.057$ (chromosome-wide $p < 0.0027$).

Since transcription is typically initiated by a complex of genes rather than a single transcription factor, we examined functional relationships among the identified upstream regulators for each hotspot (Table S7b), the genes located within a hotspot, and the genes with significant eQTL mapping to that hotspot (Table S3; *cis* eQTL significant at chromosome-wide $p < 0.01$, *trans* eQTL significant at genome-wide $p < 0.021$), using STRING v10 (Jensen *et al.* 2009, http://string-db.org/). We searched for evidence of functional relationships from experiments, databases and gene co-expression, and applied a minimum required interaction score of 0.4.

Results

Genotyping by sequencing

Sufficient numbers of reads were obtained for 620 of the 670 individuals sent for sequencing. Fifteen of these individuals failed initial quality control steps. For the 605 sticklebacks (88 parents, 517 offspring) that were retained for analysis, we obtained a total of 583,032,024 raw paired reads (40,357 – 11,940,726 per individual, median=834,286). Approximately 67% of these reads remained aligned to the stickleback genome following removal of reads with non-unique optimal alignments, any alternative suboptimal alignments, or pair-rescued alignments (range 36.2% - 78.8%, median = 70.1%). Raw read and alignment statistics for each individual are provided in Table S0.

Linkage map construction

Following SNP calling and quality control steps 13,809 of the original 25,668 SNPs, genotyped in 605 individuals (mean number of offspring per family = 18), were available for linkage map construction. Following removal of markers with < 150 informative meioses or within 500bp, 6,448 SNPS were included in the initial map build. The final sex-averaged linkage map spanned 3,110 cM Kosambi (including the complete Chromosome 19) and included 5,975 markers, of which approximately 45% were located at the same map position as another marker (Figure 1, Figure S1, Table S1). Forty-three previously un-placed scaffolds (10.35 mB) were added to the chromosome assemblies of Roesti *et al.* (2012, Table S2). Thirty-five of these scaffolds were also recently added to the stickleback assembly in an independent study by Glazer *et al.* (2015). Although there were some differences in scaffold orientation, location of the new scaffolds was almost completely congruent between the two maps (Table S2). For QTL detection with QTLMap, the map was reduced to 3,189 SNPs with unique positions (average inter-marker distance = 0.98cM, Table S1).

Identification of cis and trans eQTL

Expression data were available for 500 of the 517 genotyped offspring. Twenty-six of these offspring had > 60% missing genotype data and were removed from the analysis. As we found that missing values in the expression trait file caused QTLMap to over-estimate the LRT statistic, we eliminated these from the dataset by removing one additional individual and 195 expression traits. Eighty-eight genotyped parents, 473 genotyped and phenotyped offspring (mean no. offspring per family = 15.8, mean proportion of missing genotypes in offspring = 0.11; maximum = 0.56), and 10,332 expression traits were retained for the analysis. At chromosome-wide $p < 0.01$, we identified 5,366 eQTL associated with 4,507 expression traits (43.7% of the 10,322 expression traits examined, Table S3). Based on our recoded gene positions, we classified 2,335 of these as *cis* eQTL, 2,870 as *trans* eQTL, and 161 as unknown – that is, the expressed gene was located on a scaffold that had not been assigned to a *G. aculeatus* chromosome by either this study or Glazer *et al.* (2015; Table S3, Table S4). Four hundred and seventy four of the *trans* eQTL were significant at genome-wide $p < 0.021$. Of these, 84.5% mapped to a chromosome other than the one containing the regulated gene. After application of this genome-wide significance threshold for *trans* eQTL, 2,858 expression traits (27.7% of those examined) remained associated with one or more significant *cis* or *trans* eQTL. Of these, 79.4% were associated with a *cis* eQTL, 13.9% with one or more *trans* eQTL, 2.3% with both a *cis* and a *trans* eQTL and 4.4% with eQTL of unknown class (Table S3). The physical distribution across the genome of the 2,858 loci with significant *cis* or *trans* eQTL is shown in Figure S1. Mean 95% confidence interval of significant eQTL was 10.2 cM (range 1-86cM), approximating 1.77Mb (range 0.03 – 22.19Mb). Overall, *trans* regulated expression traits did not exhibit more dominance variance than *cis* regulated loci (*trans* regulated loci, mean $h^2 = 0.31$, mean $d^2 = 0.16$; *cis* regulated loci: mean $h^2 = 0.37$, mean $d^2 = 0.18$; values from Leder *et al.* 2015).

Trans eQTL hotspots

Trans eQTL (significant at genome wide $p < 0.021$) were not evenly distributed across the genome and we identified ten 5cM bins, located on seven different chromosomes, as containing eQTL clusters (7 or more eQTL; $p < 0.012$ based on the largest hotspot observed in neutral simulations; Figure 1). A particularly large eQTL hotspot (36 *trans* eQTL within the 5cM bin) was identified close to one end of Chromosome 6, three hotspots (23, 7, and 8 *trans* eQTL) were present at separate locations on Chromosome 12, two hotspots (10 and 7 *trans* eQTL) were located on Chromosome 4, and remaining hotspots were located near the ends of Chromosomes 7, 8, 9 and 16 (14, 10, 8 and 7 *trans* eQTL). To eliminate the possibility that distant *cis* eQTL mis-classified as *trans* were contributing to observed hotspots, we repeated the analysis with the 401 *trans* eQTL that were on a different chromosome to their regulatory target – nine out of the ten hotspots were still present (6 or more eQTL, $p < 0.038$; second Chromosome 4 hotspot, with 5 eQTL, no longer significant). Physical hotspot boundaries

were assigned from inspection of eQTL hits and 95% confidence intervals as follows: Chromosome 4, 55-67cM ('Chr4a', 4,630,680-6,394,113bp); Chromosome 4, 104-113cM ('Chr4b', 15,643,256-17,021,069bp), Chromosome 6, 111-116cM ('Chr6', 17,238,934-17,469,219bp); Chromosome 7, 5-12cM ('Chr7', 396,541-1,107,393bp); Chromosome 8, 134-139cM ('Chr8', 19,917,746-20,316,565bp); Chromosome 9, 165-174cM ('Chr9', 19,822,078-20,440,410bp); Chromosome 12, 0-1cM ('Chr12a', 0-337,849bp); Chromosome 12, 72-79cM ('Chr12b', 5,853,981-7,440,742bp); Chromosome 12, 109-119cM ('Chr12c', 15,551,555-17,229,387bp); Chromosome 16, 123-130cM ('Chr16', 17,658,526-18,257,571bp).

Genes with plastic vs. non-plastic expression

Following FDR correction, 4,253 genes were found by Leder *et al.* (2015) to exhibit a significant change in expression in response to a temperature treatment. We identified significant eQTL underlying 1131 of these genes (Table S3; eQTL type: 79.8% *cis*, 12.7% *trans*, 2.6% both, 4.9% unknown). The distribution of the 177 significant *trans* eQTL across 5cM bins indicated four hotspots (5 or more eQTL, $p < 0.01$, Figure S2), all of which had been previously observed in the full dataset. The Chromosome 16 hotspot was greatly increased in relative importance (Chr4b: 6 eQTL; Chr 6: 12 eQTL; Chr12a: 9 eQTL; Chr16: 7 eQTL).

Association of eQTL with regions under selection

None of our identified eQTL hotspots overlapped parallel regions of the genome divergent between marine and freshwater sticklebacks identified by Hohenlohe *et al.* (2010), Jones *et al.* (2012), and Terekhanova *et al.* (2014), or with the clusters of morphological QTL on Chromosome 20 (Miller *et al.* 2014, Table S5). However, one genomic region identified as divergent between marine and freshwater populations by Terekhanova *et al.* (2014) alone overlapped with the Chr12b eQTL hotspot. Only nine of the 297 genes inferred by Guo *et al.* (2015) as being under selection amongst Baltic Sea populations experiencing different temperature and salinity regimens overlapped observed eQTL hotspots (Chr4a, Chr4b, Chr7, Chr9 and Chr12b, Table S5).

Hotspot annotation

We identified human orthologues for 16,315 of the 20,787 protein-coding genes annotated on the Broad stickleback genome (78.5%, Table S4). There were 393 genes with human annotation physically located within the designated boundaries of the eleven hotspots (Table S5). Of these, 70 (17.8%) had a GO term related to transcription regulation (Table 1, Table S6). In addition, 21 genes with significant *cis* eQTL or *trans* eQTL mapping to a hotspot had GO terms related to transcriptional regulation (Table 1, Table S6). Following correction for multiple testing we found no significant GO term enrichment amongst any group of genes *trans* regulated by the same eQTL hotspot.

438 ***Upstream regulator and functional interaction analyses***

439 When examining all 405 genes with *trans* eQTL significant at genome wide p < 0.021, 79
440 significantly enriched upstream regulators were identified using IPA (Table S7). In total, these
441 regulators had 208 of the genes in the dataset as known targets. Hepatocyte nuclear factor 4α
442 (HNF4A) was identified as a particularly important regulator ($p = 9.3*10^{-8}$), with 70 (33.7%) of these
443 genes as downstream targets. Other highly enriched regulatory factors included one cut homeobox 1
444 (ONECUT1; $p = 3.2*10^{-5}$; 16 target genes), Nuclear Receptor Subfamily 4 Group A Member 1
445 (NR4A1; $p = 2.0*10^{-4}$; 11 genes), Signal Transducer And Activator Of Transcription 5B (STAT5B; p
446 $= 5.5*10^{-4}$; 10 genes), Krüppel-like factor 3 (KLF3; $p = 8.7*10^{-4}$; 15 genes), estrogen receptor 1
447 (ESR1; $p = 1.8*10^{-3}$; 37 genes); Hepatocyte nuclear factor 1α (HNF1A; $p = 1.9*10^{-3}$; 17 genes);
448 CAMP Responsive Element Binding Protein 1 (CREB1; $p=3.2*10^{-3}$; 19 genes) and myc proto-
449 oncogene protein (MYC; $p = 3.4*10^{-3}$; 30 genes). The full list of 79 significant upstream regulators is
450 in Table S7.

451 To identify upstream regulators that could be contributing to the ten eQTL hotspots we further
452 examined all genes that had *trans* eQTL mapping to the hotspots at genome-wide p< 0.057 (1120
453 genes). One hundred and ninety-two different enriched upstream regulators were identified for these
454 genes (Table S7b). For genes with *trans* eQTL mapping to the Chr4b, Chr6, Chr12a and Chr12c
455 hotspots, HNF4A remained an important regulator. Only five of the identified upstream regulators
456 were physically located within a hotspot (NFKB1, Chr4a; SOX3, Chr4a; SRF, Chr9; NFATC2,
457 Chr12b; NR4A1, Chr12b). Five had significant *cis* or *trans* eQTL mapping to a hotspot (IRF2, Chr4a
458 *trans*; NCOA4, Chr6 *cis*; HIF1A, Chr6 *trans*; JUP, Chr7 *trans*; ELK1, Chr12a *cis*). None of these ten
459 hotspot-associated regulatory proteins were identified as significant upstream regulators for the sets
460 genes with *trans* eQTL mapping to the same hotspot – in other words, their presence did not appear to
461 be causative of the observed hotspots.

462 When the enriched upstream regulators, genes with cis eQTL mapping to a hotspot at chromosome-
463 wide p < 0.01, and genes with *trans* eQTL mapping to a hotspot at genome wide p < 0.021 were
464 examined in STRING, multiple protein-protein interactions were found (Figure 2, Figure S4). In
465 particular for the Chr6 hotspot we found a complex interaction network that included eight molecules
466 *trans*-regulated by this hotspot (in order of connectivity: CTNNB1, HIF1A, CASP3, BRD8, CDK13,
467 EIF3C, JAK2, UCK1), two molecules *cis*-regulated by the hotspot (C1D and B3GNT2), and multiple
468 molecules inferred as important upstream regulators by IPA (Figure 2).

469 **Discussion**

470 In this study we identified regions of the genome underlying variation in gene expression in a
471 population of threespine stickleback from northern Europe. We used a genotyping-by-sequencing

approach to generate an improved linkage map, and applied interval mapping to identify eQTL. Our new map was independent of that recently constructed by Glazer *et al.* (2015), and the congruent placement of scaffolds between the two maps confirms the reliability of these new genome assemblies. Our map covered a substantially larger distance in cM than those of Roesti *et al.* (2013) and Glazer *et al.* (2015), probably due to differences in experimental design. Nevertheless, for our Baltic Sea population, we observe very similar patterns of recombination rate variation across and between chromosomes as found by Roesti et al. (2013) for freshwater sticklebacks from central Europe and Glazer *et al.* (2015) for marine-freshwater crosses from western North America, (Figure S1). Thus, the large scale pattern of recombination rate variation across the genome may impose, and/or be under, similar evolutionary constraints throughout the range of the species.

Using a chromosome-wide significance threshold for *cis* regulatory loci and a genome-wide threshold for *trans* loci, we identified eQTL for just over a quarter of the 10,332 expression traits examined. Because at least 74% of these expression traits exhibit significant heritable variation (Leder *et al.* 2015), and gene expression is commonly regulated by multiple eQTL, we expect that a much larger number of underlying eQTL remain undetected due to low statistical power. Despite expectations that *trans* regulatory regions might be under purifying selection due to their potentially pleiotropic effect, and that the effect of *trans* eQTL on expression will be weaker than that *cis* eQTL, we found many cases where gene expression was influenced by regulatory variation in *trans* but not in *cis*. This suggests that a frequently-used approach of detecting local selection by examining patterns of differentiation at markers linked to genes that are adaptive candidates (e.g. DeFaveri et al. 2011, Shimada et al. 2011) may fail to identify such selection as it is acting to change gene expression via *trans* regulatory regions. We did not observe any difference in additive vs dominance variance underlying genes found to be regulated in *cis* vs. those regulated in *trans*. However this may again be due to low statistical power to detect many of the underlying eQTL: genes are expected to be influenced by a large number of eQTL, meaning that the observed heritable variation is generated by a combination of additively and non-additively acting regulatory regions.

The *trans* eQTL that we detected were not randomly distributed across the genome but instead clustered into multiple eQTL hotspots. This observation is a ubiquitous feature of eQTL studies and is thought to indicate the existence of 'master regulators' acting in *trans* to influence many genes. However apparent eQTL hotspots may also arise as a statistical artefact as a result of many false positive QTL when testing thousands of expression traits in combination with spurious correlation between these traits due to uncorrected experimental factors (Wang *et al.* 2007; Breitling *et al.* 2008). Disentangling gene expression correlation that is due to common underlying regulatory architecture from that caused by experimental artefacts is a difficult analytical problem that we are unable to fully address here (Joo *et al.* 2014). Therefore, we caution that these hotspots should be verified using other stickleback populations and different approaches.

The parents for this study came from a genetically diverse marine population of threespine stickleback (DeFaveri *et al.* 2013). Local adaptation of threespine sticklebacks to freshwater has been demonstrated to arise, at least partly, from selection on standing genetic variation in the marine environment. Further, QTL underlying morphological divergence between marine and freshwater populations have been demonstrated to have pleiotropic effects (Rogers *et al.* 2012; Miller *et al.* 2014), and frequently co-localize with regions of the genome found to be under parallel selection amongst independent freshwater colonisations. One way in which these regions could exert such pleiotropic effects is by harbouring loci that influence the expression of many genes, i.e. eQTL hotspots. However, only one of the *trans* eQTL hotspots found in this study (Chr12a) overlapped with genomic regions repeatedly found to be associated with marine/freshwater divergence by Hohenlohe *et al.* (2010), Jones *et al.* (2012), or Terekhanova *et al.* (2014).

Several studies, however, indicate that adaptation to novel aquatic environments may also involve parts of the genome outside these large target regions (DeFaveri *et al.* 2011; Leinonen *et al.* 2012; Ellis *et al.* 2015; Ferchaud and Hansen 2016; Erickson *et al.* 2016). The QTL underlying physiological adaptations to different aquatic environments in sticklebacks have not been well characterized. Recently, Kusakabe *et al* (2016) identified a significant QTL associated with salinity tolerance (indicated by gill sodium plasma levels) on Chromosome 16, which overlaps our Chr16 *trans* eQTL hotspot. Interestingly, this also appears to overlap with a Chromosome 16 QTL underlying gill raker morphology identified by Glazer *et al* (2015). Based on transcription levels, Kusakabe *et al* (2016) identified ten candidate causal genes at the QTL location; we found *cis* regulatory variation for four of these genes (CLN5, IGFBP5, RABL3, NDUFA10) and a fifth (GDP-like) had a *trans* eQTL mapping to the Chr4a hotspot. However, Kusakabe *et al* (2016) did not investigate genes located elsewhere on the genome that may be trans-regulated by this Chromosome 16 QTL. Our results also show that all genes with *trans* eQTL mapping to the Chr16 hotspot exhibit a plastic response to the temperature treatment. Thus, the Chr 16 eQTL hotspot may be involved in physiological adjustment to several environmental variables.

Identifying eQTL directly implicated in local adaptation in sticklebacks was not our experimental aim, and it is possible that regulatory hotspots acting in tissues or life stages that we did not examine have a role in stickleback adaptive radiation. In general, it is difficult to predict in which tissues, or at which life stages, gene expression variation gives rise to observed adaptive differences. We examined transcription in the liver, an easily accessible, metabolically active, tissue. The liver expresses many genes with potential roles in the physiological adaptation to different aquatic environments, including hormone receptors and genes involved in osmoregulation, energy homeostasis, and response to hypoxia. Further, many eQTL identified in this study may be common to other tissues. In general, the extent to which eQTL are shared amongst tissues remains unclear, due to the need for very large sample sizes and the limitations of the statistical methodologies available to address this question

(The GTEx Consortium 2015). In particular, variation in gene expression levels amongst tissues means that the power to detect underlying eQTL also varies amongst tissues. Although studies have suggested that up to 70% of genes may have common underlying eQTL across tissues (Nica *et al.* 2011), there is also some evidence that *trans* eQTL hotspots in particular may act in a tissue-specific manner (Grundberg *et al*. 2012). Thus, replication of this study in a greater range of tissues, and at different life stages, would shed more light on the regulatory genetic architecture underlying the parallel changes observed when marine sticklebacks independently colonize freshwater.

To investigate the potential genetic mechanisms generating the nine observed eQTL hotspots we searched for associated loci with known transcriptional regulatory functions, and performed upstream regulator analysis for the genes with eQTL in the hotspots. Although the pathways regulating transcription are still poorly characterized for most genes, particularly in non-mammalian species, these analyses can provide useful preliminary information. We found no evidence that eQTL hotspots were due to the presence of a single 'master' regulatory locus, or a cluster of regulatory genes, at the hotspot locations. Although many genes with roles in transcriptional regulation were present in, or regulated by, hotspots, finding such genes is not unexpected: approximately 18% of the human orthologues of BROAD stickleback genes are annotated with the GO terms that we used to identify transcriptional regulators. It is also possible that the regulatory elements generating such hotspots are not annotated coding genes: microRNAs and long non-coding RNAs are potentially important *trans* regulators (Vance and Ponting 2014) and not yet well characterized across the stickleback genome.

Our results suggest that, alternatively, these hotspots may be generated by a complex interaction of multiple transcription regulators. Several well-characterized regulatory proteins were identified as important upstream regulators for genes with *trans* eQTL mapping to the hotspots. Unsurprisingly, these included three genes - HNF4A, ONECUT1 and HNF1A - known to be master transcriptional regulators in the mammalian liver (Odom *et al*. 2004). HNF4A and ONECUT1 were identified as a particularly strongly enriched upstream regulators when examining all genes with a *trans* eQTL at genome-wide $p<0.021$ (Table S7), and were also found to be enriched when examining the subsets of genes with *trans* eQTL mapping to the hotspots on Chromosome 4, Chromosome 6, and Chromosome 12 (Table S7). None of the three genes were physically located in any hotspot, and we were unable to identify significant eQTL underlying variation in their expression (ONECUT1 was not on the microarray). However, we note that HNF4A is less than 300 kb from hotspot Chr12b. These regulators likely act through direct and indirect interactions with other proteins to regulate transcription. Interacting molecules that are especially of interest in respect to hotspot locations are hypoxia inducible factor 1α and catenin beta-1 (HIF1A & CTNNB1, *trans* regulated by the Chr6 hotspot, Fig. 2), histone deacetylase 3 (HDAC3, located in the Chr4b hotspot, Fig. S4), and vitamin D receptor (VDR, located in the Chr12c hotspot, Fig. S4).

579 The protein HIF1A has previously been investigated as a selective target of local adaptation in fish. It
580 is part of a transcriptional complex (HIF) that alters the expression of numerous genes in many tissues
581 in response to low oxygen conditions (Nikinmaa and Rees 2005, Liu *et al*. 2013). It is also involved in
582 temperature adaptation in fish (Rissanen *et al.* 2006; Liu *et al.* 2013). Thus, HIF1A is of relevance
583 when fish colonize aquatic environments with differing oxygen regimens, for example benthic vs.
584 limnetic habitats or different areas of the Baltic Sea. Rytkönen *et al.* (2007) found no association
585 between variation in the HIF1A coding region and adaptation to hypoxic conditions across various
586 fish species, and markers linked to HIF1A do not appear be under directional selection amongst Baltic
587 Sea stickleback populations (Shimada *et al.* 2011); however the gene was recently found to be under
588 positive selection in high-altitude loach lineages (Wang *et al.* 2015). HIF1A is known to be
589 transcriptionally regulated in fish (Liu *et al.* 2013), and our identification of a *trans* eQTL for HIF1A
590 demonstrates that regulatory variation for this gene is present in Baltic Sea sticklebacks and could be
591 an alternative, unexamined, target of selection. The proteins HNF4A, CNNB1 and HDAC3 are also
592 involved in the hypoxia response (Xu *et al.* 2011; Wang *et al.* 2015).

593 In conclusion, we have performed the first genome-wide characterisation of the regulatory
594 architecture of gene expression in *G. aculeatus.* We found that variation in gene expression was
595 influenced by polymorphism in both *cis*-acting and *trans* acting regulatory regions. Trans-acting
596 eQTLS clustered into hotspots. In general these hotspots did not co-locate with regions of the genome
597 known to be associated with parallel adaptive divergence among marine and freshwater threespine
598 sticklebacks. However, one hotspot overlapped with a known QTL underlying salinity tolerance, a
599 locally adaptive trait. Hotspots locations appeared to be mediated by complex interactions amongst
600 regulator molecules rather than the presence of few 'master regulators'. Our broad-scale study
601 suggests many avenues for finer-scale investigation of the role of transcriptional regulation in
602 stickleback evolution.

603 **Data accessibility**

604 Raw and normalized microarray data, in addition to R scripts describing the normalization procedure,
605 are available in the ArrayExpress database (www.ebi.ac.uk/arrayexpress) under accession number E-
606 MTAB-3098. RAD sequence reads for each individual have been deposited in the NCBI Sequence
607 Read Archive under BioProject ID PRJNA340327. Input files and scripts will be deposited in
608 DRYAD.

609 **Acknowledgements**

610 This work was funded by grants from Academy of Finland to C.P., E.L., M. N. and J.M. (grant nos.
611 129662, 134728, 133875, 136464, 141231, 250435 and 265211). Tiina Sävilammi wrote the script for

612 barcode splitting and we thank her for bioinformatics advice. We also thank the numerous people who
613 helped in obtaining and maintaining sticklebacks. Generous computing resources were provided by
614 the Finnish Centre for Scientific Computing (CSC-IT). Research was conducted under an ethical
615 license from the University of Helsinki (HY121-06). Comments from two anonymous reviewers
616 greatly improved the manuscript.

617 **References**

618 Anderson E. C., 2012 Large-scale parentage inference with SNPs: an efficient algorithm for statistical
619 confidence of parent pair allocations. Stat. Appl. Genet. Mol. Biol. **11**.

620 Ayroles J. F., Carbone M. A., Stone E. A., Jordan K. W., Lyman R. F., Magwire M. M., *et al*. 2009
621 Systems genetics of complex traits in *Drosophila melanogaster*. Nat. Genet. **41**: 299–307.

622 Barreto F. S., Moy G. W., Burton R. S., 2011 Interpopulation patterns of divergence and selection
623 across the transcriptome of the copepod *Tigriopus californicus*. Mol. Ecol. **20**: 560–572.

624 Barrett R. D. H., Paccard A., Healy T. M., Bergek S., Schulte P. M., Schluter D., Rogers S. M., 2011
625 Rapid evolution of cold tolerance in stickleback. Proc. Biol. Sci. **278**: 233–238.

626 Bernatchez L., Renaut S., Whiteley A. R., Derome N., Jeukens J., Landry L., *et al.* 2010 On the origin
627 of species: insights from the ecological genomics of lake whitefish. Philos. Trans. R. Soc. Lond.
628 B. Biol. Sci. **365**: 1783–1800.

629 Breitling R., Li Y., Tesson B. M., Fu J., Wu C., Wiltshire T., *et al*. 2008 Genetical genomics:
630 spotlight on QTL hotspots. PLoS Genet. **4**: e1000232.

631 Carbon, S., Ireland, A., Mungall, C. J., Shu, S., Marshall, B., Lewis, S., AmiGO Hub, Web Presence
632 Working Group, 2009. AmiGO: online access to ontology and annotation data. Bioinformatics.
633 25: 288-289.

634 Chan Y. F., Marks M. E., Jones F. C., Villarreal G., Shapiro M. D., Brady S. D., *et al.* 2010 Adaptive
635 evolution of pelvic reduction in sticklebacks by recurrent deletion of a Pitx1 enhancer. Science
636 **327**: 302–305.

637 Chaturvedi A., Raeymaekers J. A. M., Volckaert F. A. M., 2014 Computational identification of
638 miRNAs, their targets and functions in three-spined stickleback (*Gasterosteus aculeatus*). Mol.
639 Ecol. Resour. **14**: 768–777.

640 Clément-Ziza M., Marsellach F. X., Codlin S., Papadakis M. A., Reinhardt S., Rodríguez-López M.,

et al. 2014 Natural genetic variation impacts expression levels of coding, non-coding, and antisense transcripts in fission yeast. Mol. Syst. Biol. **10**: 764.

Cleves, P. A., Ellis, N. A., Jimenez, M. T., Nunez, S. M., Schluter, D., Kingsley, D. M., Miller, C. T. 2014 . Evolved tooth gain in sticklebacks is associated with a cis-regulatory allele of Bmp6. Proc. Natl. Acad. Sci. USA **111:** 13912-13917.

Colosimo P. F., Hosemann K. E., Balabhadra S., Villarreal G., Dickson M., Grimwood J., *et al.* 2005 Widespread parallel evolution in sticklebacks by repeated fixation of Ectodysplasin alleles. Science **307**: 1928–1933.

Conte G. L., Arnegard M. E., Best J., Chan Y. F., Jones F. C., Kingsley D. M., *et al.* 2015 Extent of QTL reuse during repeated phenotypic divergence of sympatric threespine stickleback. Genetics **201**: 1189–200.

Cubillos F. A., Coustham V., Loudet O., 2012 Lessons from eQTL mapping studies: non-coding regions and their role behind natural phenotypic variation in plants. Curr. Opin. Plant Biol. **15**: 192–198.

Danecek P., Auton A., Abecasis G., Albers C. A., Banks E., DePristo M. A., *et al.* 2011 The variant call format and VCFtools. Bioinformatics **27**: 2156–2158.

DeFaveri J., Jonsson P. R., Merilä J., 2013 Heterogeneous genomic differentiation in marine threespine sticklebacks: adaptation along an environmental gradient. Evolution **67**: 2530–2546.

DeFaveri J., Shikano T., Shimada Y., Goto A., Merilä J., 2011 Global analysis of genes involved in freshwater adaptation in threespine sticklebacks (*Gasterosteus aculeatus*). Evolution **65**: 1800–1807.

Di-Poï C., Bélanger, D., Amyot, M. Rogers, S., Aubin-Horth, N. 2016. Receptors rather than signals change in expression in four physiological regulatory networks during evolutionary divergence in threespine stickleback. Mol. Ecol. **25**: 3416–3427

Durbin M. L., Lundy K. E., Morrell P. L., Torres-Martinez C. L., Clegg M. T., 2003 Genes that determine flower color: the role of regulatory changes in the evolution of phenotypic adaptations. Mol. Phylogenet. Evol. **29**: 507–518.

Durinck S., Moreau Y., Kasprzyk A., Davis S., Moor B. De, Brazma A., Huber W., 2005 BioMart and Bioconductor: a powerful link between biological databases and microarray data analysis. Bioinformatics **21**: 3439–3440.

671 Ellis N. A., Glazer A. M., Donde N. N. *et al. (*2015*)* Distinct developmental genetic mechanisms
672 underlie convergently evolved tooth gain in sticklebacks. Development **142:** 2442–2451.

673 Ellison C. K., Burton R. S., 2008 Genotype-dependent variation of mitochondrial transcriptional
674 profiles in interpopulation hybrids. Proc. Natl. Acad. Sci. U. S. A. **105**: 15831–15836.

675 Elsen J.-M., Mangin B., Goffinet B., Boichard D., Roy P. Le, 1999 Alternative models for QTL
676 detection in livestock. I. General introduction. Genet. Sel. Evol. **31**: 213.

677 Elshire R. J., Glaubitz J. C., Sun Q., Poland J. A., Kawamoto K., Buckler E. S., Mitchell S. E., 2011 A
678 robust, simple genotyping-by-sequencing (GBS) approach for high diversity species. PLoS One
679 **6**: e19379.

680 Erickson P. A., Glazer A. M., Killingbeck E. E., Agoglia R. M., Baek J., Carsanaro S. M., Lee A. M.,
681 Cleves P. A., Schluter D. and Miller C. T. (2016), Partially repeatable genetic basis of benthic
682 adaptation in threespine sticklebacks. *Evolution* **70:** 887–902

683 Ferchaud A.-L., Hansen M. M., 2016 The impact of selection, gene flow and demographic history on
684 heterogeneous genomic divergence: threespine sticklebacks in divergent environments. Mol.
685 Ecol. **25**: 238–295.

686 Flint J., Mackay T. F. C., 2009 Genetic architecture of quantitative traits in mice, flies, and humans.
687 Genome Res. **19**: 723–733.

688 Glazer A. M., Killingbeck E. E., Mitros T., Rokhsar D. S., Miller C. T., 2015 Genome assembly
689 improvement and mapping convergently evolved skeletal traits in sticklebacks with genotyping-
690 by-sequencing. G3 **5**: 1463–1472.

691 Green, P., Falls, K., Crooks, S. 1990. Documentation for CRI-MAP, version 2.4. Washington
692 University School of Medicine, St. Louis, MO.

693 Gruber J. D., Vogel K., Kalay G., Wittkopp P. J., 2012 Contrasting properties of gene-specific
694 regulatory, coding, and copy number mutations in *Saccharomyces cerevisiae*: frequency, effects,
695 and dominance. PLoS Genet. **8**: e1002497.

696 Grundberg E., Small K. S., Hedman A. K., Nica A. C., Buil A., Keildson S., Bell J. T., Yang T. P.,
697 Meduri E., Barrett A., *et al.* 2012. Mapping cis- and trans-regulatory effects across multiple
698 tissues in twins. Nat Genet **44**: 1084–1089

699 Guerrero R. F, Posto A. L., Moyle L. C., Hahn, M. W., 2016 Genome-wide patterns of regulatory
700 divergence revealed by introgression lines. Evolution **70**: 696-706.

Guo B., DeFaveri J., Sotelo G., Nair A., Merilä J., 2015 Population genomic evidence for adaptive differentiation in Baltic Sea three-spined sticklebacks. BMC Biol. **13**: 19.

Hines H. M., Papa R., Ruiz M., Papanicolaou A., Wang C., Nijhout H. F., *et al*. 2012 Transcriptome analysis reveals novel patterning and pigmentation genes underlying *Heliconius* butterfly wing pattern variation. BMC Genomics **13**: 288.

Hohenlohe P. A., Bassham S., Etter P. D., Stiffler N., Johnson E. A., Cresko W. A., 2010 Population genomics of parallel adaptation in threespine stickleback using sequenced RAD tags. PLoS Genet. **6**: e1000862.

Huang D. W., Sherman B. T., Lempicki R. A., 2009a Systematic and integrative analysis of large gene lists using DAVID bioinformatics resources. Nat. Protoc. **4**: 44–57.

Huang D. W., Sherman B. T., Lempicki R. A., 2009b Bioinformatics enrichment tools: paths toward the comprehensive functional analysis of large gene lists. Nucleic Acids Res. **37**: 1–13.

Huang Y., Chain F. J. J., Panchal M., Eizaguirre C., Kalbe M., *et al*, 2016, Transcriptome profiling of immune tissues reveals habitat-specific gene expression between lake and river sticklebacks. Mol Ecol. **25:** 943–958.

Jensen L. J., Kuhn M., Stark M., Chaffron S., Creevey C., Muller J., *et al.* 2009. STRING 8 - a global view on proteins and their functional interactions in 630 organisms. Nucleic Acids Res. **37**: D412-6.

Johnsson M., Jonsson K. B., Andersson L., Jensen P., Wright D., 2015 Genetic regulation of bone metabolism in the chicken: similarities and differences to Mammalian systems. PLoS Genet. **11**: e1005250.

Jones F. C., Grabherr M. G., Chan Y. F., Russell P., Mauceli E., Johnson J., Swofford R., *et al*. 2012 The genomic basis of adaptive evolution in threespine sticklebacks. Nature **484**: 55–61.

Joo J. W. J., Sul J. H., Han B., Ye C., Eskin E., 2014 Effectively identifying regulatory hotspots while capturing expression heterogeneity in gene expression studies. Genome Biol. **15**: r61.

Kitano J., Lema S. C., Luckenbach J. A., Mori S., Kawagishi Y., Kusakabe M., Swanson P., Peichel C.L. 2010. Adaptive divergence in the thyroid hormone signaling pathway in the stickleback radiation. Curr. Biol. **20:** 2124-2130.

Knott S. A., Elsen J. M., Haley C. S., 1996 Methods for multiple-marker mapping of quantitative trait loci in half-sib populations. Theor. Appl. Genet. **93**: 71–80.

731 Konijnendijk N., Shikano T., Daneels D., Volckaert F. A. M., Raeymaekers J. A. M., 2015 Signatures
732 of selection in the three-spined stickleback along a small-scale brackish water - freshwater
733 transition zone. Ecol. Evol. **5**: 4174-4186

734 Kusakabe M., Ishikawa A., Ravinet M., Yoshida K., Makino T., Toyoda A., Fujiyama A., Kitano, J.
735 (2016), Genetic basis for variation in salinity tolerance between stickleback ecotypes. Mol Ecol.
736 Accepted Author Manuscript. doi:10.1111/mec.13875

737 Lai Z., Gross B. L., Zou Y., Andrews J., Riesberg L. H., 2006 Microarray analysis reveals differential
738 gene expression in hybrid sunflower species. Mol. Ecol. **15**: 1213–1227.

739 Landry C. R., Wittkopp P. J., Taubes C. H., Ranz J. M., Clark A. G., Hartl D. L., 2005 Compensatory
740 cis-trans evolution and the dysregulation of gene expression in interspecific hybrids of
741 *Drosophila*. Genetics **171**: 1813–1822.

742 Leder E. H., McCairns R. J. S., Leinonen T., Cano J. M., Viitaniemi H. M., Nikinmaa M., *et al*. 2015
743 The evolution and adaptive potential of transcriptional variation in sticklebacks--signatures of
744 selection and widespread heritability. Mol. Biol. Evol. **32**: 674–689.

745 Leder E., Merilä J., Primmer C., 2009 A flexible whole-genome microarray for transcriptomics in
746 three-spine stickleback (*Gasterosteus aculeatus*). BMC Genomics **10**: 426.

747 Leinonen T., Cano J., Merilä J., 2011 Genetics of body shape and armour variation in threespine
748 sticklebacks. J. Evol. Biol. **24**: 206–218.

749 Leinonen T., McCairns R. J. S., Herczeg G., Merilä J., 2012 Multiple evolutionary pathways to
750 decreased lateral plate coverage in freshwater threespine sticklebacks. Evolution **66**: 3866–3875.

751 Lescak E. A., Bassham S. L., Catchen J., Gelmond O., Sherbick M. L., Hippel F. A. von, Cresko W.
752 A., 2015 Evolution of stickleback in 50 years on earthquake-uplifted islands. Proc. Natl. Acad.
753 Sci. USA **112**: E7204–E7212.

754 Li H., Durbin R., 2009 Fast and accurate short read alignment with Burrows-Wheeler transform.
755 Bioinformatics **25**: 1754–1760.

756 Li H., Handsaker B., Wysoker A., Fennell T., Ruan J., Homer N., *et al.* 2009 The Sequence
757 Alignment/Map format and SAMtools. Bioinformatics **25**: 2078–2079.

758 Liu J., Shikano T., Leinonen T., Cano J. M., Li M.-H., Merilä J., 2014 Identification of major and
759 minor QTL for ecologically important morphological traits in three-spined sticklebacks
760 (*Gasterosteus aculeatus*). G3 **4**: 595–604.

761 Liu S., Zhu K., Chen N., Wang W., Wan H., 2013 Identification of HIF-1α promoter and expression
762 regulation of HIF-1α gene by LPS and hypoxia in zebrafish. Fish Physiol. Biochem. **39**: 1153-
763 1163

764 Mackay T. F. C., Stone E. A., Ayroles J. F., 2009 The genetics of quantitative traits: challenges and
765 prospects. Nat. Rev. Genet. **10**: 565–577.

766 Mäkinen H. S., Cano J. M., Merilä J., 2006 Genetic relationships among marine and freshwater
767 populations of the European three-spined stickleback (*Gasterosteus aculeatus*) revealed by
768 microsatellites. Mol. Ecol. **15**: 1519–1534.

769 Mallarino R., Grant P. R., Grant B. R., Herrel A., Kuo W. P., Abzhanov A., 2011 Two developmental
770 modules establish 3D beak-shape variation in Darwin's finches. Proc. Natl. Acad. Sci. U. S. A.
771 **108**: 4057–4062.

772 McCairns R. J. S., Bernatchez L., 2010 Adaptive divergence between freshwater and marine
773 sticklebacks: insights into the role of phenotypic plasticity from an integrated analysis of
774 candidate gene expression. Evolution **64**: 1029–1047.

775 Mecham B. H., Nelson P. S., Storey J. D., 2010 Supervised normalization of microarrays.
776 Bioinformatics **26**: 1308–1315.

777 Meiklejohn C. D., Coolon J. D., Hartl D. L., Wittkopp P. J., 2014 The roles of cis- and trans-
778 regulation in the evolution of regulatory incompatibilities and sexually dimorphic gene
779 expression. Genome Res. **24**: 84–95.

780 Metzger B. P. H, Duveaum F., Yuan, D. C., Tryban, S., Yang, B., Wittkopp, P. J., 2016. Contrasting
781 frequencies and effected of cis- and trans- regulatory mutations affecting gene expression. Mol.
782 Biol. Evol. **33:** 1131-1146.

783 Miller C. T., Glazer A. M., Summers B. R., Blackman B. K., Norman A. R., Shapiro M. D., *et al.*
784 2014 Modular skeletal evolution in sticklebacks is controlled by additive and clustered
785 quantitative trait loci. Genetics **197**: 405–420.

786 Morris M. R. J., Richard R., Leder E. H., Barrett R. D. H., Aubin-Horth N., Rogers S. M., 2014 Gene
787 expression plasticity evolves in response to colonization of freshwater lakes in threespine
788 stickleback. Mol. Ecol. **23**: 3226–3240.

789 Mudunuri, U., Che, A., Yi, M., Stephens, R. M. 2009. bioDBnet: the biological database network.
790 Bioinformatics **25**:555-556.

Nica A.C., Parts L., Glass D., Nisbet J., Barrett A., Sekowska M., *et al.* 2011. The architecture of gene regulatory variation across multiple human tissues: The MuTHER study. PLoS Genet 7: e1002003.

Nikinmaa M., Rees B. B., 2005 Oxygen-dependent gene expression in fishes. Am. J. Physiol. Regul. Integr. Comp. Physiol. **288**: R1079–1090.

Odom, D. T., Zizlsperger, N., Gordon, D. B., Bell, G. W., Rinaldi, N. J., Murray, H. L., *et al.* 2004. Control of pancreas and liver gene expression by HNF transcription factors. Science **303**: 1378-1381.

Pavey S. A., Collin H., Nosil P., Rogers S. M., 2010 The role of gene expression in ecological speciation. Ann. N. Y. Acad. Sci. **1206**: 110–129.

Peichel C. L., Ross J. A., Matson C. K., Dickson M., Grimwood J., Schmutz J., Myers R. M., Mori S., Schluter D.,Kingsley, D. M., 2004 The master sex-determination locus in threespine sticklebacks is on a nascent Y chromosome. Curr. Biol. **14:** 1416-1424.

Poelstra J. W., Vijay N., Hoeppner M. P., Wolf J. B. W., 2015 Transcriptomics of colour patterning and colouration shifts in crows. Mol. Ecol. **24**: 4617–4628.

Powell J. E., Henders A. K., McRae A. F., Kim J., Hemani G., Martin N. G., *et al.* 2013 Congruence of additive and non-additive effects on gene expression estimated from pedigree and SNP data. PLoS Genet. **9**: e1003502.

Purcell S., Neale B., Todd-Brown K., Thomas L., Ferreira M. A. R., Bender D., *et al.* 2007 PLINK: a tool set for whole-genome association and population-based linkage analyses. Am. J. Hum. Genet. **81**: 559–575.

R Core Team 2015. R: a language and environment for statistical computing.Vienna, Austria: R Foundation for Statistical Computing.

Reed R. D., Papa R., Martin A., Hines H. M., Counterman B. A., Pardo-Diaz C., *et al.* 2011 Optix drives the repeated convergent evolution of butterfly wing pattern mimicry. Science **333**: 1137–1141.

Rennison D. J., Owens G. L., Heckman N., Schluter D., Veen T. 2016. Rapid adaptive evolution of colour vision in the threespine stickleback radiation. Proc. R. Soc. B **283** DOI: 10.1098/rspb.2016.0242

Rissanen E., Tranberg H. K., Sollid J., Nilsson G. E., Nikinmaa M., 2006 Temperature regulates

hypoxia-inducible factor-1 (HIF-1) in a poikilothermic vertebrate, crucian carp (*Carassius carassius*). J. Exp. Biol. **209**: 994–1003.

Roesti M., Hendry A. P., Salzburger W., Berner D., 2012 Genome divergence during evolutionary diversification as revealed in replicate lake-stream stickleback population pairs. Mol. Ecol. **21**: 2852–2862.

Roesti M., Kueng B., Moser D., Berner D., 2015 The genomics of ecological vicariance in threespine stickleback fish. Nat. Commun. **6**: 8767.

Roesti M., Moser D., Berner D., 2013 Recombination in the threespine stickleback genome--patterns and consequences. Mol. Ecol. **22**: 3014–3027.

Rogers S. M., Tamkee P., Summers B., Balabahadra S., Marks M., Kingsley D. M., Schluter D., 2012 Genetic signature of adaptive peak shift in threespine stickleback. Evolution **66**: 2439–2450.

Rytkönen K. T., Vuori K. A. M., Primmer C. R., Nikinmaa M., 2007 Comparison of hypoxia-inducible factor-1 alpha in hypoxia-sensitive and hypoxia-tolerant fish species. Comp. Biochem. Physiol. Part D. Genomics Proteomics **2**: 177–186.

Schaefke B., Emerson J. J., Wang T.-Y., Lu M.-Y. J., Hsieh L.-C., Li W.-H., 2013 Inheritance of gene expression level and selective constraints on trans- and cis-regulatory changes in yeast. Mol. Biol. Evol. **30**: 2121–2133.

Schluter D., McPhail J. D., 1992 Ecological character displacement and speciation in sticklebacks. Am. Nat. **140**: 85–108.

Schultheiß R., Viitaniemi H. M., Leder E. H., 2015 Spatial dynamics of evolving dosage compensation in a young sex chromosome system. Genome Biol. Evol. **7**: 581–590.

Shimada Y., Shikano T., Merilä J., 2011 A high incidence of selection on physiologically important genes in the three-spined stickleback, *Gasterosteus aculeatus*. Mol. Biol. Evol. **28**: 181–193.

Smedley D., Haider S., Ballester B., Holland R., London D., Thorisson G., Kasprzyk A., 2009 BioMart--biological queries made easy. BMC Genomics **10**: 22.

Steige K. A., Laenen B., Reimegård J., Scofield D., Slotte T., 2015 The impact of natural selection on the distribution of cis-regulatory variation across the genome of an outcrossing plant. BioRxiv.

Taylor E. B., McPhail J. D., 2000 Historical contingency and ecological determinism interact to prime speciation in sticklebacks, *Gasterosteus*. Proc. Biol. Sci. **267**: 2375–2384.

Terekhanova N. V, Logacheva M. D., Penin A. A., Neretina T. V, Barmintseva A. E., Bazykin G. A., *et al.* 2014 Fast evolution from precast bricks: genomics of young freshwater populations of threespine stickleback *Gasterosteus aculeatus*. PLoS Genet. **10**: e1004696.

The GTEx Consortium, 2015. The genotype-tissue expression (GTEx) pilot analysis: Multitissue gene regulation in humans. Science **348:** 648-660.

Turner L. M., White M. A., Tautz D., Payseur B. A., 2014 Genomic networks of hybrid sterility. PLoS Genet. **10**: e1004162.

van Nas A., Ingram-Drake L.,Sinsheimer J. A., Wang S. S., Schadt E. E., Drake T., Lusis A. J., 2010, Expression quantitative trait loci: replication, tissue- and sex-specificity in mice. Genetics **185:** 1059–1068

Vance K. W., Ponting C. P., 2014 Transcriptional regulatory functions of nuclear long noncoding RNAs. Trends Genet. **30**: 348–355.

Wang S., Zheng T., Wang Y., 2007 Transcription activity hot spot, is it real or an artifact? BMC Proc. **1 Suppl 1**: S94.

Wang Y., Yang L., Zhou K., Zhang, Y., Song, Z., He, S. 2015. Evidence for adaptation to the Tibetan plateau Inferred from Tibetan loach transcriptomes. Genome Biol. Evol. **7**: 2970–2982.

Whiteley A. R., Derome N., Rogers S. M., St-Cyr J., Laroche J., Labbe A., *et al.* 2008 The phenomics and expression quantitative trait locus mapping of brain transcriptomes regulating adaptive divergence in lake whitefish species pairs (*Coregonus* sp.). Genetics **180**: 147–164.

Wickham, H. 2009 *ggplot2: Elegant Graphics for Data Analysis*. Springer New York.

Willert K., Jones, K. A. 2006. Wnt signaling: Is the party in the nucleus? Genes Dev **20:**1394–1404

Wu C., Delano D. L., Mitro N., Su S. V, Janes J., McClurg P., *et al*. 2008 Gene set enrichment in eQTL data identifies novel annotations and pathway regulators. PLoS Genet. **4**: e1000070.

Xu, H., Lu, A., Sharp, F. R. (2011) Regional genome transcriptional response of adult mouse brain to hypoxia. BMC Genomics **12**:499

Zhang X., Cal A. J., Borevitz J. O., 2011 Genetic architecture of regulatory variation in *Arabidopsis thaliana*. Genome Res. **21**: 725–733.

878 **Table 1:** Known transcriptional regulators associated with identified eQTL hotspots. Human orthologues of stickleback genes were identified using BioMart.
879 Location is as follows: 'Hotspot': annotated gene is in genomic region of hotspot; '*Cis*': gene is cis-regulated by hotspot at chromosome wide p<0.01;
880 '*Trans*': gene is trans-regulated by hotspot at genome-wide p<0.021.

Hotspot	Location	Stickleback Ensembl_ID	Human Ensembl_ID	Gene Name	Description
Chr04a	Cis	ENSGACG00000017632	ENSG00000133884	DPF2	double PHD fingers 2
Chr04a	Cis	ENSGACG00000017819	ENSG00000156603	MED19	mediator complex subunit 19
Chr04a	Cis	ENSGACG00000017706	ENSG00000168002	POLR2G	polymerase (RNA) II subunit G
Chr04a	Cis	ENSGACG00000017981	ENSG00000155827	RNF20	ring finger protein 20
Chr04a	Hotspot	ENSGACG00000017062	ENSG00000175602	CCDC85B	coiled-coil domain containing 85B
Chr04a	Hotspot	ENSGACG00000017113	ENSG00000131264	CDX4	caudal type homeobox 4
Chr04a	Hotspot	ENSGACG00000016877	ENSG00000145214	DGKQ	diacylglycerol kinase theta
Chr04a	Hotspot	ENSGACG00000016862	ENSG00000088881	EBF4	early B-cell factor 4
Chr04a	Hotspot	ENSGACG00000016923	ENSG00000126500	FLRT1	fibronectin leucine rich transmembrane protein 1
Chr04a	Hotspot	ENSGACG00000017059	ENSG00000175592	FOSL1	FOS like 1, AP-1 transcription factor subunit
Chr04a	Hotspot	ENSGACG00000017029	ENSG00000184481	FOXO4	forkhead box O4
Chr04a	Hotspot	ENSGACG00000016896	ENSG00000161021	MAML1	mastermind like transcriptional coactivator 1
Chr04a	Hotspot	ENSGACG00000016876	ENSG00000109320	NFKB1	nuclear factor kappa B subunit 1
Chr04a	Hotspot	ENSGACG00000017076	ENSG00000174576	NPAS4	neuronal PAS domain protein 4
Chr04a	Hotspot	ENSGACG00000017018	ENSG00000123728	RAP2C	RAP2C, member of RAS oncogene family
Chr04a	Hotspot	ENSGACG00000017237	ENSG00000147274	RBMX	RNA binding motif protein, X-linked
Chr04a	Hotspot	ENSGACG00000017181	ENSG00000134595	SOX3	SRY-box 3
Chr04a	Hotspot	ENSGACG00000016868	ENSG00000131508	UBE2D2	ubiquitin conjugating enzyme E2 D2
Chr04a	Hotspot	ENSGACG00000016930	ENSG00000185670	ZBTB3	zinc finger and BTB domain containing 3

Chr04a	Hotspot	ENSGACG00000017211	ENSG00000152977	ZIC1	Zic family member 1
Chr04a	Hotspot	ENSGACG00000017212	ENSG00000156925	ZIC3	Zic family member 3
Chr04a	Trans	ENSGACG00000019192	ENSG00000105856	HBP1	HMG-box transcription factor 1
Chr04a	Trans	ENSGACG00000018763	ENSG00000168310	IRF2	interferon regulatory factor 2
Chr04a	Trans	ENSGACG00000010116	ENSG00000163904	SENP2	SUMO1/sentrin/SMT3 specific peptidase 2
Chr04a	Trans	ENSGACG00000019776	ENSG00000234495	TRIM27	tripartite motif containing 27
Chr04b	Hotspot	ENSGACG00000018659	ENSG00000112983	BRD8	bromodomain containing 8
Chr04b	Hotspot	ENSGACG00000018605	ENSG00000198791	CNOT7	CCR4-NOT transcription complex subunit 7
Chr04b	Hotspot	ENSGACG00000018730	ENSG00000170619	COMMD5	COMM domain containing 5
Chr04b	Hotspot	ENSGACG00000018655	ENSG00000147257	GPC3	glypican 3
Chr04b	Hotspot	ENSGACG00000018752	ENSG00000171720	HDAC3	histone deacetylase 3
Chr04b	Hotspot	ENSGACG00000018614	ENSG00000179111	HES7	hes family bHLH transcription factor 7
Chr04b	Hotspot	ENSGACG00000018626	ENSG00000101928	MOSPD1	motile sperm domain containing 1
Chr04b	Hotspot	ENSGACG00000018642	ENSG00000156531	PHF6	PHD finger protein 6
Chr04b	Hotspot	ENSGACG00000018664	ENSG00000138814	PPP3CA	protein phosphatase 3 catalytic subunit alpha
Chr04b	Hotspot	ENSGACG00000018680	ENSG00000185129	PURA	purine rich element binding protein A
Chr04b	Hotspot	ENSGACG00000018663	ENSG00000184584	TMEM173	transmembrane protein 173
Chr04b	Trans	ENSGACG00000018210	ENSG00000121060	TRIM25	tripartite motif containing 25
Chr04b	Trans	ENSGACG00000001351	ENSG00000116830	TTF2	transcription termination factor 2
Chr06	Cis	ENSGACG00000012317	ENSG00000266412	NCOA4	Nuclear receptor coactivator 4
Chr06	Cis	ENSGACG00000001371	ENSG00000167380	ZNF226	Zinc finger protein 226
Chr06	Hotspot	ENSGACG00000011981	ENSG00000197223	C1D	C1D nuclear receptor co-repressor
Chr06	Trans	ENSGACG00000018659	ENSG00000112983	BRD8	Bromodomain containing 8
Chr06	Trans	ENSGACG00000005983	ENSG00000168036	CTNNB1	Catenin (cadherin-associated protein), beta 1, 88kDa
Chr06	Trans	ENSGACG00000004982	ENSG00000065883	CDK13	Cyclin-dependent kinase 13
Chr06	Trans	ENSGACG00000008525	ENSG00000100644	HIF1A	Hypoxia inducible factor 1, alpha subunit
Chr06	Trans	ENSGACG00000013704	ENSG00000096968	JAK2	Janus kinase 2

Chr06	Trans	ENSGACG00000009631	ENSG00000107938	EDRF1	erythroid differentiation regulatory factor 1
Chr06	Trans	ENSGACG00000018816	ENSG00000196670	ZFP62	ZFP62 zinc finger protein
Chr07	Cis/Hotspot	ENSGACG00000018669	ENSG00000137462	TLR2	Toll-like receptor 2
Chr07	Hotspot	ENSGACG00000000325	ENSG00000135625	EGR4	Early growth response 4
Chr07	Hotspot	ENSGACG00000018606	ENSG00000109670	FBXW7	F-box And WD repeat domain containing 7, E3 ubiquitin protein ligase
Chr07	Hotspot	ENSGACG00000000304	ENSG00000170448	NFXL1	Nuclear transcription factor, X-box binding-like 1
Chr07	Hotspot	ENSGACG00000000370	ENSG00000164985	PSIP1	PC4 and SFRS1 interacting protein 1
Chr07	Hotspot	ENSGACG00000018586	ENSG00000074966	TXK	Tyrosine kinase
Chr07	Trans	ENSGACG00000000333	ENSG00000173801	JUP	Junction plakoglobin
Chr08	Hotspot	ENSGACG00000014457	ENSG00000162733	DDR2	Discoidin domain receptor tyrosine kinase 2
Chr08	Hotspot	ENSGACG00000014404	ENSG00000187764	SEMA4D	Sema domain, immunoglobulin domain (Ig), transmembrane domain (TM) and short cytoplasmic domain, (Semaphorin) 4D
Chr08	Hotspot	ENSGACG00000014374	ENSG00000178078	STAP2	signal transducing adaptor family member 2
Chr08	Trans	ENSGACG00000006033	ENSG00000125686	MED1	Mediator complex subunit 1
Chr08	Trans	ENSGACG00000017475	ENSG00000137699	TRIM29	tripartite motif containing 29
Chr08	Trans	ENSGACG00000003512	ENSG00000148204	CRB2	crumbs 2, cell polarity complex component
Chr08	Trans	ENSGACG00000006901	ENSG00000136999	NOV	nephroblastoma overexpressed
Chr09	Cis	ENSGACG00000019842	ENSG00000128272	ATF4	activating transcription factor 4
Chr09	Cis	ENSGACG00000019868	ENSG00000103423	DNAJA3	DnaJ heat shock protein family (Hsp40) member A3
Chr09	Hotspot	ENSGACG00000019898	ENSG00000162961	DPY30	Dpy-30 histone methyltransferase complex regulatory subunit
Chr09	Hotspot	ENSGACG00000019915	ENSG00000132664	POLR3F	Polymerase (RNA) III (DNA directed) polypeptide F, 39 KDa
Chr09	Hotspot	ENSGACG00000020002	ENSG00000112658	SRF	Serum response factor
Chr09	Hotspot	ENSGACG00000019873	ENSG00000011243	AKAP8L	A-kinase anchoring protein 8 like
Chr12a	Cis	ENSGACG00000000816	ENSG00000126767	ELK1	ELK1, member of ETS oncogene family
Chr12a	Hotspot	ENSGACG00000000295	ENSG00000146109	ABT1	Activator of basal transcription 1
Chr12a	Hotspot	ENSGACG00000000248	ENSG00000106785	TRIM14	Tripartite motif containing 14

Chr12a	Trans	ENSGACG00000019625	ENSG00000164134	NAA15	N(Alpha)-acetyltransferase 15, NatA auxiliary subunit
Chr12a	Trans	ENSGACG00000001088	ENSG00000111581	NUP107	Nucleoporin 107kDa
Chr12b	Cis	ENSGACG00000006074	ENSG00000185513	L3MBTL1	L(3)mbt-like
Chr12b	Cis	ENSGACG00000004938	ENSG00000012504	NR1H4	Nuclear receptor subfamily 1, group h, member 4
Chr12b	Hotspot	ENSGACG00000011155	ENSG00000101017	CD40	CD40 molecule, TNF receptor superfamily member 5
Chr12b	Hotspot	ENSGACG00000010943	ENSG00000110925	CSRNP2	Cysteine-serine-rich nuclear protein 2
Chr12b	Hotspot	ENSGACG00000011240	ENSG00000163349	HIPK1	Homeodomain interacting protein kinase 1
Chr12b	Hotspot	ENSGACG00000011086	ENSG00000101096	NFATC2	Nuclear factor of activated T-cells, cytoplasmic, calcineurin-dependent 2
Chr12b	Hotspot	ENSGACG00000010788	ENSG00000123358	NR4A1	Nuclear receptor subfamily 4, group A, member 1
Chr12b	Hotspot	ENSGACG00000010925	ENSG00000184271	POU6F1	POU class 6 homeobox 1
Chr12b	Hotspot	ENSGACG00000010838	ENSG00000181852	RNF41	Ring finger protein 41, E3 ubiquitin protein ligase
Chr12b	Hotspot	ENSGACG00000011124	ENSG00000101115	SALL4	Spalt-like transcription factor 4
Chr12b	Hotspot	ENSGACG00000011135	ENSG00000182463	TSHZ2	Teashirt zinc finger homeobox 2
Chr12b	Hotspot	ENSGACG00000010929	ENSG00000135457	TFCP2	Transcription factor CP2
Chr12b	Hotspot	ENSGACG00000011187	ENSG00000204859	ZBTB48	Zinc finger and BTB domain containing 48
Chr12b	Hotspot	ENSGACG00000011128	ENSG00000020256	ZFP64	Zinc finger protein 64
Chr12b	Hotspot	ENSGACG00000010636	ENSG00000126895	AVPR2	arginine vasopressin receptor 2
Chr12b	Hotspot	ENSGACG00000011168	ENSG00000171680	PLEKHG5	pleckstrin homology and RhoGEF domain containing G5
Chr12b	Hotspot	ENSGACG00000011023	ENSG00000134242	PTPN22	protein tyrosine phosphatase, non-receptor type 22
Chr12b	Trans	ENSGACG00000011682	ENSG00000162761	LIMX1A	LIM homeobox transcription factor 1, alpha
Chr12c	Cis	ENSGACG00000013344	ENSG00000101997	CCDC22	Coiled-coil domain containing 22
Chr12c	Cis	ENSGACG00000013103	ENSG00000196924	FLNA	Filamin A, alpha
Chr12c	Cis	ENSGACG00000005361	ENSG00000116670	MAD2L2	Mitotic spindle assembly checkpoint protein MAD2B
Chr12c	Cis/Hotspot	ENSGACG00000004839	ENSG00000188157	AGRN	Agrin
Chr12c	Hotspot	ENSGACG00000004256	ENSG00000101126	ADNP	Activity-dependent neuroprotector homeobox
Chr12c	Hotspot	ENSGACG00000004544	ENSG00000009307	CSDE1	Cold shock domain containing E1, RNA-binding

Chr12c	Hotspot	ENSGACG00000004732	ENSG00000101412	E2F1	E2F transcription factor 1
Chr12c	Hotspot	ENSGACG00000004740	ENSG00000078747	ITCH	Itchy E3 ubiquitin protein ligase
Chr12c	Hotspot	ENSGACG00000004213	ENSG00000197780	TAF13	TAF13 RNA Polymerase II, TATA box binding protein (TBP)-associated factor, 18kDa
Chr12c	Hotspot	ENSGACG00000004773	ENSG00000122691	TWIST2	Twist homolog 2
Chr12c	Hotspot	ENSGACG00000004763	ENSG00000111424	VDR	Vitamin D (1,25- dihydroxyvitamin D3) receptor
Chr12c	Hotspot	ENSGACG00000004734	ENSG00000131061	ZNF341	Zinc finger protein 341
Chr12c	Hotspot	ENSGACG00000004662	ENSG00000197114	ZGPAT	Zinc finger, CCCH-type with G patch domain
Chr12c	Hotspot	ENSGACG00000004338	ENSG00000088832	FKBP1A	FK506 Binding Protein 1A
Chr16	Cis	ENSGACG00000005831	ENSG00000153234	NR4A2	Nuclear receptor subfamily 4, group A, member 2
Chr16	Trans	ENSGACG00000012487	ENSG00000125845	BMP2	Bone morphogenetic protein 2

881 **Figure Legend**

882 **Figure 1** Position of SNP markers along each chromosome (top) and location of *trans* eQTL hits for
883 all assayed genes (bottom). Black bars show the number of eQTL hits at each 1cM Kosambi interval
884 along the chromosome. Blue shading shows the number of eQTL with 95% confidence intervals
885 overlapping each 1cM interval. Arrows indicate the location of eight significant *trans* eQTL hotspots.
886 Figure created using ggplot2 (Wickham 2009) in R.

887 **Figure 2:** Networks of known protein-protein interactions inferred by String 10 for proteins
888 associated with the Chr6 hotspot. 'Upstream Regulator': significantly enriched upstream regulator
889 identified when examining genes *trans*-regulated by the hotspot using IPA; 'Hotspot Location':
890 protein is coded by a gene physically located in the hotspot; 'Trans regulated': protein is *trans*
891 regulated by an eQTL mapping to the hotspot and significant at genome-wide $p<0.021$; Cis/Hotspot:
892 both present in and significantly *cis* regulated by the hotspot. Interactions not involving an identified
893 upstream regulator are not shown.

894

Figure 1

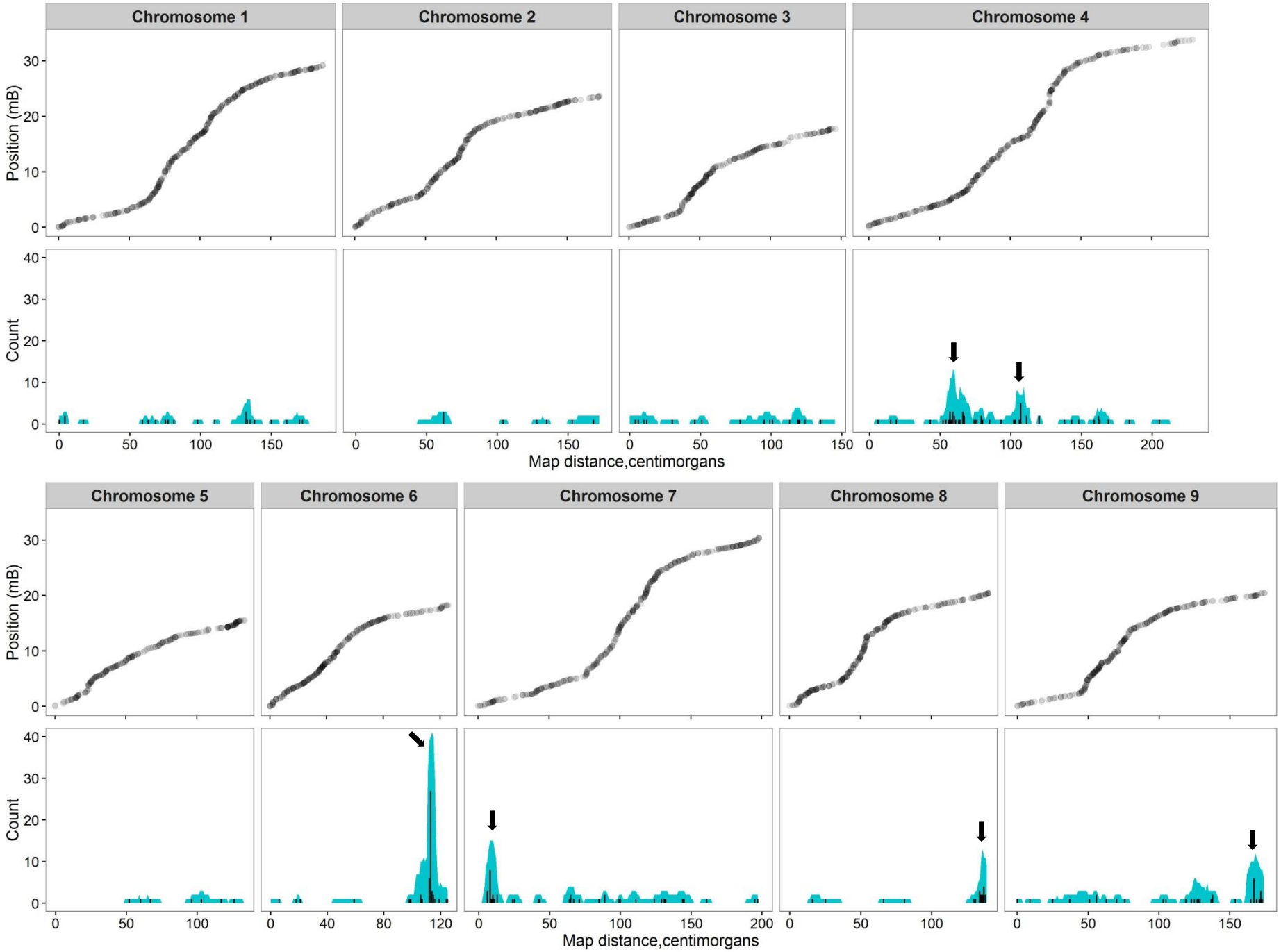
Chromosome 1
Chromosome 2
Chromosome 3
Chromosome 4
Chromosome 5
Chromosome 6
Chromosome 7
Chromosome 8
Chromosome 9
Position (mB)
Count
Map distance,centimorgans

Figure 1 (cont.)

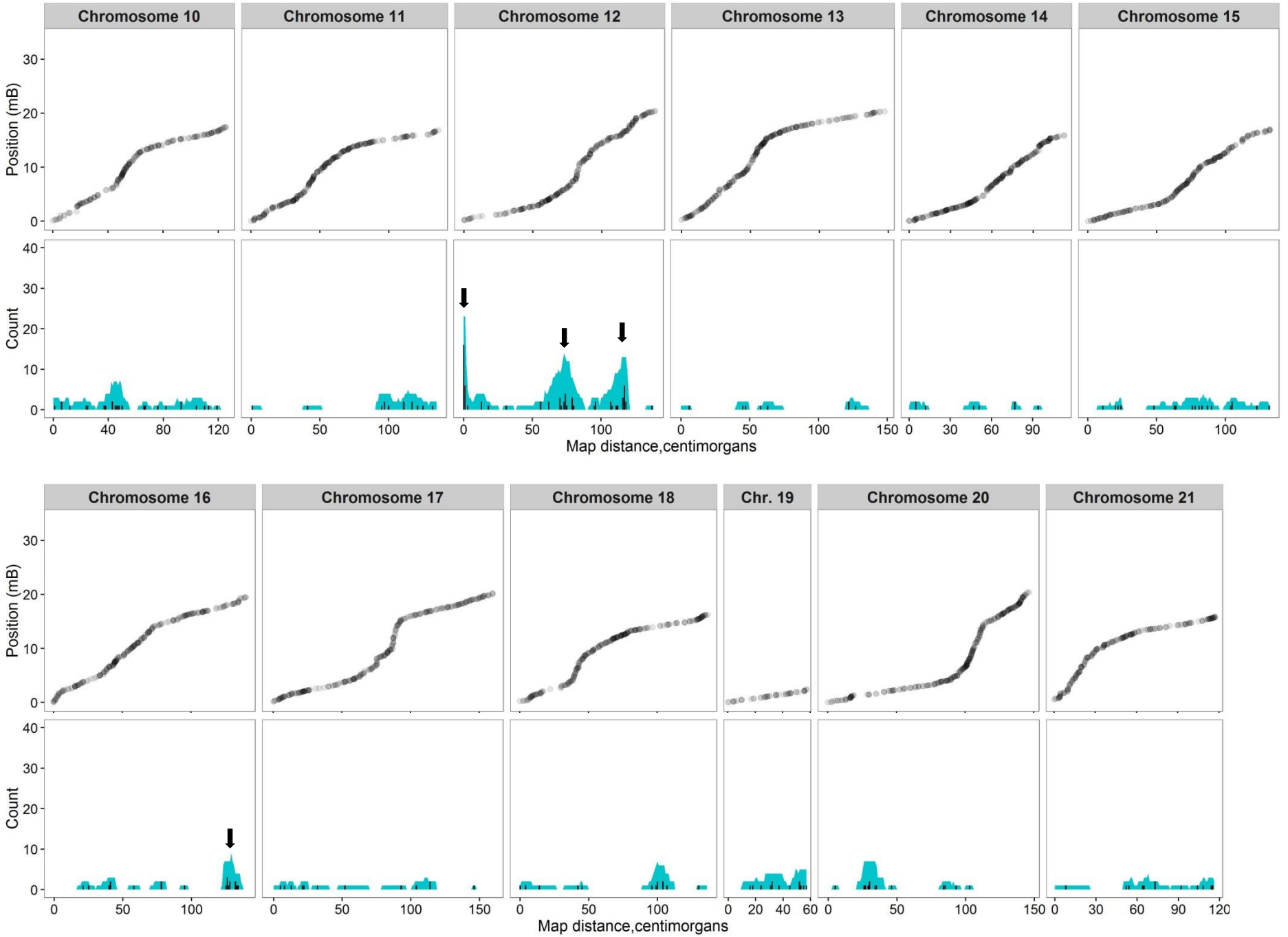

Figure 2